INTERNATIONAL JOURNAL OF AUTOMOTIVE AND MECHANICAL ENGINEERING
ISSN: 2229-8649 e-ISSN: 2180-1606
VOL. 21, ISSUE 2, 2024, 11287 – 11301
DOI: https://doi.org/10.15282/ijame.21.2.2024.9.0872

RESEARCH ARTICLE

Numerical Study on the Effect of Incorporating Phase Change Materials in a Wall

M. Aidi[1,2]*, Y. Harnane[1,2], S. Bouzid[1,2], L. Bordja[1,2]

[1]University of Oum El Bouaghi, Faculty of Sciences and Applied Sciences, Department of Mechanical Engineering, Algeria
[2]Laboratory of Advanced Design and Modeling of Mechanical Systems and Thermo-Fluid (CMASMTF), University of Oum El Bouaghi, Algeria

ABSTRACT - Integrating phase-change materials (PCMs) into the structure of a building can significantly improve its heat storage capacity and thermal performance. Thanks to their phase-change properties, PCMs can absorb, store and release large amounts of energy in the form of latent heat within a narrow temperature range. This study examines the thermal behavior of a housing wall that incorporates PCM to increase its thermal inertia. Simulations using Ansys Fluent 14.0 software compare a standard wall with a wall incorporating layers of PCM of different thicknesses and positions. Three types of PCM - RT28 kerosene, $C_aCl_2.6H_2O$ wet salt and A26 - are evaluated. The results show that positioning the PCM layer on the interior surface adjacent to the indoor environment can reduce internal heat flow by around 50% compared with a standard wall. In addition, the study identifies an optimum PCM layer thickness of between 10 and 15 cm.

ARTICLE HISTORY
Received : 24th May 2023
Revised : 11th Jan. 2024
Accepted : 17th May 2024
Published : 20th June 2024

KEYWORDS
Phase change material
Numerical modeling
Thermal inertia
Thermal behavior

1.0 INTRODUCTION

The construction sector significantly contributes to global energy consumption and greenhouse gas emissions, accounting for 25% of total global energy consumption. In 2010, the IEA (International Energy Agency) reported that the building industry was the third largest energy consumer after manufacturing and transport industries. Moreover, the building energy field alone accounted for 40% of global energy resource consumption and a third of global greenhouse gas emissions, mainly due to the energy used for lighting, heating, cooling, and air conditioning. The construction sector's energy consumption is expected to rise in the coming years due to rapid urbanization and increasing demand for infrastructure development. This trend is compounded by the fact that fossil fuels dominate the global energy market. Forecasts predict that petroleum and coal will keep supplying 75-80% of global energy by 2030 and will be the world's primary energy source[1]-[3]. In Algeria, the national consumption of energy absorbed by the construction sector (residential and tertiary) varies from 26% to 45% depending on the region, the sector's energy consumption, with an average annual growth rate of 12% [3], is primarily attributed to the lighting, heating, cooling, and air conditioning of buildings, and this consumption rate is expected to rise as the country continues to experience population growth and urbanization. The use of petroleum and coal in the building industry is not only environmentally unsustainable but also economically unsustainable. The global need to save energy has become a critical issue, especially after the energy crisis of the 1970s. European countries were particularly affected, leading them to accelerate their efforts towards energy independence. Energy conservation in buildings has been a primary focus of these efforts, and many solutions have been proposed to minimize energy use in the construction sector. One effective method is the application of PCM in heating and cooling systems [4]-[10]. PCM technology can reduce energy consumption in two ways: passively, by incorporating PCM into building materials to increase thermal mass and minimize internal temperature fluctuations, thus reducing heating and cooling demands, and actively, by using PCM in thermal or cold storage units. Alternatively, an active strategy entails employing PCM to store heat for subsequent use, allowing the building's thermal mass to absorb and release energy more efficiently. Due to the importance of this field, many investigations have been done by researchers as published in the literature.

Jingchao Xie et al. [11] conducted a study into the thermal efficiency of buildings using PCM wall panels. Their research revealed that a building fitted with a PCM wall panel featuring a wider phase transition span utilized 103 kilojoules less energy in June than a standard wall panel. They concluded that the thermal behavior of PCM wall panels could fluctuate over the seasons and stressed the importance of analyzing thermal performance throughout the year. In addition, they sought to determine the months in which the phase shift significantly influenced the thermal performance of the wall. The authors employed the heat ratio. Pengcheng Wang et al. [12]. An adapted building roof is proposed. (ABR) that incorporated shape-shifting transparency phase change material (VTSS-PCM) to enhance energy usage in buildings. According to their findings, the ABR design might minimize heat acquired by 35.250%compared to a standard thermal insulation roof. The authors identified the depths of the VTSS-PCM, the VTSS-PCM's extinction coefficient in the clear state, and the whiteness of the mirroring film as the three major variables affecting the ABR's performance. Soares et al.[13].

***CORRESPONDING AUTHOR | M. Aidi** | ✉ aidi.moussa@univ-oeb.dz

In Coimbra, Portugal, a study was carried out to demonstrate the feasibility of integrating phase-change materials (PCMs) into the structural cells of shading components linked to south-facing windows. The aim of this integration was to capture sun-powered heat for interior heating in wintertime. To numerically design and parametrically optimize a heat storage system utilizing latent energy, the researchers used a two-dimensional simulation model based on enthalpic composition. The research revealed that solar radiation flux significantly affected the charge melting process due to the inadequacy of the latent heat storage system at ambient temperature. Kaushik Biswas et al. [14]. Simulations were carried out utilizing a recently validated two-dimensional wall model with a (PCM) layer and HFMA enthalpy functions. The scientists altered the wall model to account for the looping phenomena seen in PCMs, which is characterized by varying PCM melt and thawing temperatures. The results showed statistically significant differences in the thermal efficiency of a standard wall compared with a wall with a PCM stratum. These results underline the need to take into account the phenomenon of hysteresis in the design of PCM-based heat retention systems.

Kissock JK and colleagues conducted simulation research in Dayton, Ohio, using simulated weather data. The outcomes of their study indicated that incorporating 10% K18 concrete into concrete walls can decrease 19% in maximum cross-wall cooling loads and a 13% decrease in annual cross-wall cooling loads [15], [16]. An examination of the current literature reveals that the main focus is on various forms of composite walls based on PCMs, in particular wall panels (e.g., plasterboard or drywall) and PCM-based concrete composites. These include alternative building blocks and containers made from PVC or aluminum foil. [17]-[19]. The various methods of incorporating PCM into building materials generally fall into several categories, encompassing direct integration and immersion in selected materials and partial and total encapsulation [19].

Direct consolidation has proved effective for integrating PCM into load-bearing materials like plaster and concrete. Its disadvantages include the absence of protective barriers, making the system vulnerable to PCM leakage during dissolution and chemical reactions with the carrier materials [18], [20]. PCM leaks present additional risks, making the system flammable and incompatible with building materials. An alternative is to pack PCMs completely into containers such as bags, tubes or sheets before incorporating them into composite walls [4], [19]. However, the encapsulation of aggregates poses problems related to temperature variances between the center and the edges of the PCM, which may result in partial melting or solidification of the phase-change materials [4], [19], [21]. Concrete appears to be an ideal candidate due to its intrinsically high thermal inertia properties. Concrete, whose volumetric thermal effect and capacity are superior to plasterboard due to its higher density, offers promising potential [22].

Encapsulation of PCM prior to incorporation into concrete has been suggested as a preventive measure against infiltration. However, research by Hunger et al. indicates a 13% reduction in the crushing resistance of the chosen mix [23]. Compaction of concrete can have a negative effect on thermal conductivity [19], which can affect its effective response to temperature changes. To optimize the use of PCM, it is suggested that they be layered, for example, by using wallpaper filled with PCM [24]-[28] or placed in large insulated containers against the wall. It should be noted that previous research has mainly placed the PCM layer adjacent to the indoor setting hunger [24]-[28]. However, other locations have also been studied, such as the outside of the wall [29]. Previous experience confirms the significant impact of placing the PCM inside the walls of a building on the phase change process and the improvement of heat efficiency [30]. It should be stressed that most previous studies have focused on a single type of phase-change material.

Given the challenges posed by the placement and choice of PCM type, this research aims to design an energy-efficient building envelope featuring PCM technology in the form of insulated layers adjacent to concrete. The objective is to decrease energy usage and enhance thermal efficiency. Numerical studies are presented using the commercial software "Fluent 14.0" and the analysis of a reference wall and a wall composed of a layer of PCM and a layer of ordinary concrete under identical thermal conditions. Three types of PCM - kerosene RT28, hydrosalt $CaCl_2.6H_2O$ and A26 - were investigated and analyzed at different PCM locations to determine the optimal location to ensure thermal comfort. In addition, the study explores the optimal thickness of a PCM layer compared with a layer of ordinary concrete under identical thermal conditions.

2.0 NUMERICAL MODELING

During the phase change process, certain phenomena occur, including thermal absorption or release of energy within a specific range at an almost constant temperature. The presence of a moving boundary, which separates the two phases where the absorption or release of thermal energy occurs, can also be observed. This information is relevant to the study of phase change processes and can aid in understanding the physical changes that occur during these processes.

2.1 Geometric Configurations and Boundary Conditions

In this research paper, two case studies (numerical studies) were undertaken to examine the thermal performance of external walls in a living environment. The first case study involved a reference wall with dimensions of 50 cm in width and 2.4 m in height, representing the external wall of a habitat. The external face of the wall was subjected to a constant heat flow, which was uniformly distributed over the entire face. In contrast, the internal face exchanged heat with the interior air by natural convection. This case study is depicted in Figure 1(a). The second PCM was placed in the external part of the wall, while the second layer was a normal concrete wall with a thickness of 40 cm. This case study is illustrated in Figure 1(b). Both case studies were subjected to identical boundary conditions.

2.2 Thermophysical Properties

This study explores the performance of two types of walls under identical initial and boundary conditions. The first wall is a 50 cm thick concrete wall, whose specific thermo-physical properties are provided in Table 1. The unsteady energy equation is numerically solved for a time interval of $\Delta t = 1\ s$ over 12 hours of 43200 s. The second wall is a compound wall that incorporates phase change materials (PCM). This wall comprises a 40 cm thick normal concrete layer and a 10 cm thick PCM layer. Table 1 lists the thermo-physical parameters of the PCM materials used in this investigation. The energy equation, accounting for phase change, is numerically solved in the unsteady regime for $\Delta t = 1\ s$ over the same 12-hour period of 43200 s.

Table 1. Thermal properties of the PCMs selected for this study

Type PCM	Description	T of Melting *[°C]*	Latent Heat [*KJ/Kg*]	Specific Heat, Cp, [*J/Kg.K*]	Thermal Conductivity, K [*W/m.K*]	Density [Kg/m^3]
Paraffin (Organic)	RT28 (Octadecan) $C_{18}H_{38}$	28.2	245	2140 (Solid 15°*C*)/ 2660 (Liquid30°*C*)	0.35 (Solid) 0.149 (Liquid)	814 (Solid) 775 (Liquid)
Salt (Inorganic)	$CaCl_2 \cdot 6H_2O$ (Calcium Chloride) (Hexa-Hydrate)	29	188,34	1400(Solid 24°*C*)/ 2310(Liquid32°*C*)	1.09(Solid23°*C*)/ 0.54(Liquid 38,7°*C*)	1802(Solid24°*C*) /1562(Liquid 32°*C*)
Fatty acid (Organic)	A26 $CH_3 (CH_2)_{2n}COOH$	26	2220	2220	0.21	790
Wall	Normal Concrete			880	1.4	2300

3.0 MATHEMATICAL MODEL

The melting process in the PCM was modeled and simulated using the ANSYS (Fluent) 14.0 program. To depict solidification and melting, the program adopts the enthalpy porosity approach [31]. Rather than explicitly tracking the merging interface, this technique allocates a liquid percentage to every unit within the phase change material area, reflecting the proportion of the liquid cell volume. After each repetition, the liquid fraction is computed using the enthalpy balance. The phase-shifting interface is represented by a pasty region where the percentage of liquid increases from 0 to 1. As the material solidifies, this pasty zone functions as a pseudo- or porous zone, with porosity gradually decreasing from 1 to 0. When solidification is complete, the porosity is zero, and the velocity increases.

Simulation assumptions

The assumptions made during the numerical modeling are as follows:

1. Fusion is unsteady and two-dimensional
2. PCM is assumed to be uniform and uniform in all directions
3. Fluid is Newtonian and incompressible.
4. Heat transfer throughout the wall is by conduction
5. The flow of PCM in its liquid phase is laminar.
6. PCM's density, viscosity, and thermal conductivity change linearly with temperature.
7. No heat generation in the PCM.

3.1 Convective Transfer in the Building

The convective transfer Within the structure is generally qualified, in the absence of any external mechanical action (air conditioner, fan), as natural. This type of transfer involves an interior convective exchange coefficient hint, and the heat flow Amid the interior areas wall and the interior Edifice environment is written using Newton's law as follows:

$$\boldsymbol{\phi_{cv,p} = h_{int}(T_{si,p} - T_{int})} \quad (1)$$

where

$\boldsymbol{\phi_{cv,p}}$ Wall interior convective flow density

$\boldsymbol{h_{int}}$ Interior convective exchange coefficient

$\mathbf{T_{si,p}}$ Interior wall surface temperature

$\mathbf{T_{int}}$ Interior air temperature

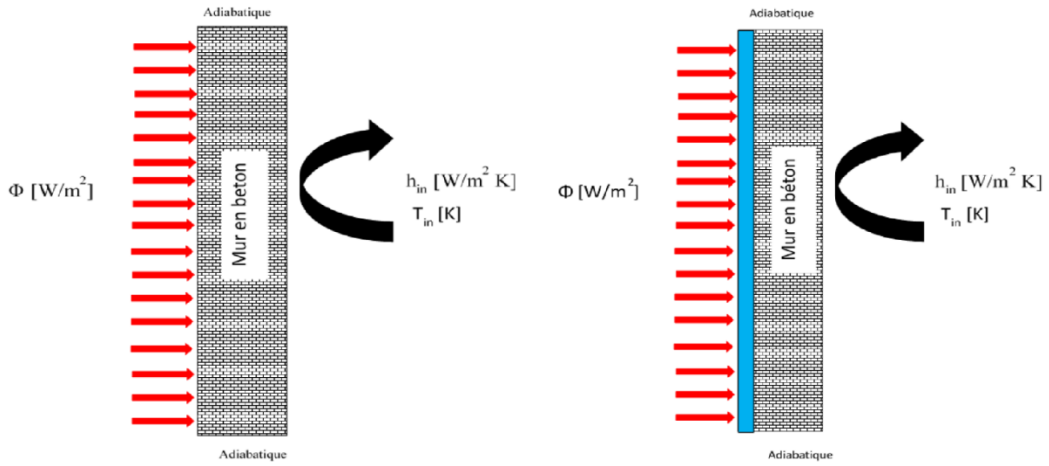

(a) Wall of reference (b) Wall with PCM

Figure 1. Study configurations

3.2 *Density of Daily Flow*

During a period corresponding to the established regime, the daily energy consumption $\phi Journalier$ is calculated from the flow density at the inner face of the wall:

$$\boldsymbol{\phi_{Daily} = \int_{time} h_{int}(T(x = L) - T_{int})dt} \quad (2)$$

This quantity expressed in (kWh/m²) reflects the accumulation of the densities of the instantaneous on the internal face.

3.3 *The Relative Difference in Energy Consumption*

The findings are reproduced concerning the relative disparity in energy consumption between a wall equipped with PCM and the reference wall, as follows:

$$\boldsymbol{\sigma = \left[\phi_{Daily}^{PCM} - \phi_{Daily}^{ref} \Big/ \phi_{Daily}^{ref}\right] \times 100} \quad (3)$$

3.4 *Governing Equations*

The conservation of energy equation solved in the fluent code:

$$\boldsymbol{\frac{\partial(\rho H)}{\partial t} = \nabla \cdot (\rho \vec{v} H) - \nabla \cdot (k \cdot \nabla T) + (S)} \quad (4)$$

where

$\boldsymbol{H}$: enthalpy; ρ the density; v the fluid velocity and S the source term

$\boldsymbol{\frac{\partial}{\partial t}(\rho H)}$ Overall energy content of the fluid within the control volume

$\boldsymbol{\nabla \cdot (\rho \vec{v} H)}$ Includes the consideration of energy transfer resulting from fluid movement into and out of the control volume (convection)

$\boldsymbol{\nabla \cdot (k \cdot \nabla T)}$ Incorporates heat transfer through conduction across the surfaces of the control volume

$\boldsymbol{S}$ takes into account other sources of energy such as chemical reactions, electric current,

L'enthalpie $\boldsymbol{H}$ est calculée comme la somme de la chaleur sensible et latente

$$H = h + \Delta H \quad (5)$$

where $\boldsymbol{h}$ represents the sensible enthalpy at a specific point and time, and $\Delta \boldsymbol{H}$ denotes the latent heat.

$$\boldsymbol{h = h_{ref} + \int_{T_{ref}}^{T} c_p dT} \quad (6)$$

where

$\boldsymbol{h_{ref}}$ Is the baseline (reference) enthalpy,

$\boldsymbol{T_{ref}}$ Is the baseline (reference) temperature

$\boldsymbol{c_p}$ represents the specific heat at constant pressure of the PCM.

$$\Delta H = \beta \, \boldsymbol{L} \tag{7}$$

where $\boldsymbol{\beta}$ is the value of the liquid fraction, and L is the latent heat of the PCM. The value of the latent heat is zero when the material is solid **($\boldsymbol{\beta}$ =0**) and equal to $\boldsymbol{L}$ when the material is liquid **($\boldsymbol{\beta}$ =1).**

$\boldsymbol{\beta = 0} \quad \rightarrow \quad \boldsymbol{T < T_{Solid}}$

$\boldsymbol{\beta = 1} \quad \rightarrow \quad \boldsymbol{T > T_{Liquid}}$

$\boldsymbol{\beta = \frac{T - T_{solid}}{T_{liquid} - T_{solid}}} \quad \rightarrow \quad \boldsymbol{T_{Solid} < T < T_{liquid}}$

$\boldsymbol{T_{solid}}$ and $\boldsymbol{T_{liquid}}$ are properties of the material [31] − [33]

The envelope is subjected to a constant heat flow on the external wall for 12 hours while the internal temperature is kept constant, allowing internal thermal comfort [34], [35] and the internal heat exchange coefficient. Table 2 shows details of the mesh and boundary conditions.

Table 2. Mesh details and boundary conditions

Boundary conditions		Structured and regular mesh	
Left wall	Heat flux $\phi = 350 W/m^2$	Width	Height
Right wall	Heat convection $h_{in} = 10\ W/m^2K$ $Tin = 23°C$	90	150
Top wall	adiabatic		
Bottom wall	adiabatic		

4.0 RESULTS AND DISCUSSION

4.1 Mesh and Resolution Tools

The geometry is rectangular, and the neat and regular grid is suitable for differentiation. The mesh was generated using Gambit software (2.4), Table 2. Figure 2 depicts the resulting mesh.

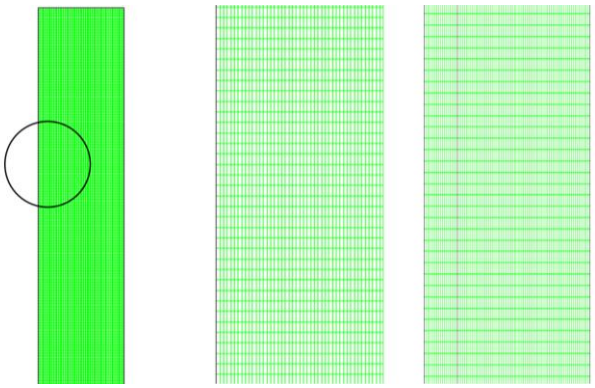

Figure 2. 2D wall mesh

The objective of this study is to investigate the resolution of the energy equation. The investigation will utilize the computational fluid dynamics (CFD) software "Fluent 14.0" to simulate and analyze the studied phenomena. The Second Order Upwind discretization scheme has been employed as it is considered the most suitable for simulating phase change. The implicit Euler scheme has been utilized for temporal discretization. The SIMPLE algorithm was used to obtain the numerical solution of the energy equation, which includes the initial and boundary conditions for all study cases. Despite selecting the implicit solving method, the influence of time step size on the results has been evaluated by testing time steps of both 0.1 seconds and 0.5 seconds, which did not affect the results. The simulations were carried out using a 1 s time step for a duration of 12 hours, representing a day from 6:00 am to 6:00 pm.

4.2 Numerical Validation

To validate the precision of the computational fluid dynamics (CFD) model, Hannon et al. [36], under the influence of the Degree of warmth temperature between the hot and cold wall, heat transfer occurs towards the PCM, which increases its temperature and causes it to melt Figure 3. Figure 4 shows the liquid fraction's development over time for the reference solution superimposed on the solution obtained using our computer code (commercial software “Fluent 14.0”). A close overlap is noted between the results of the standard study and current studies' results, with a relative difference in the liquid fraction of less than 3%.

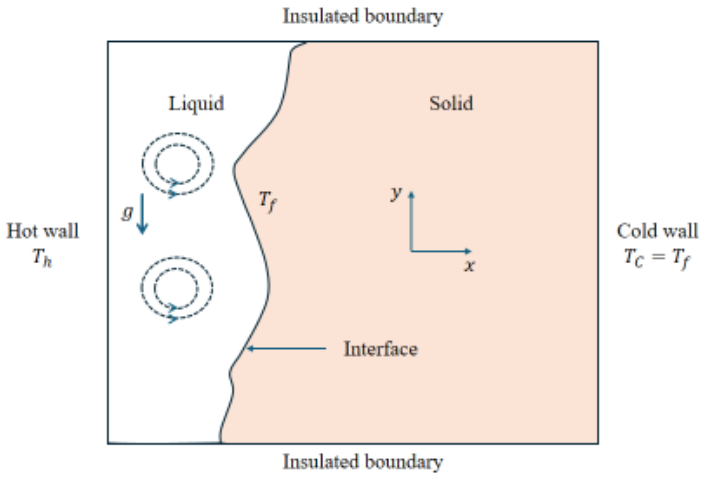

Figure 3. Study geometry of [22]

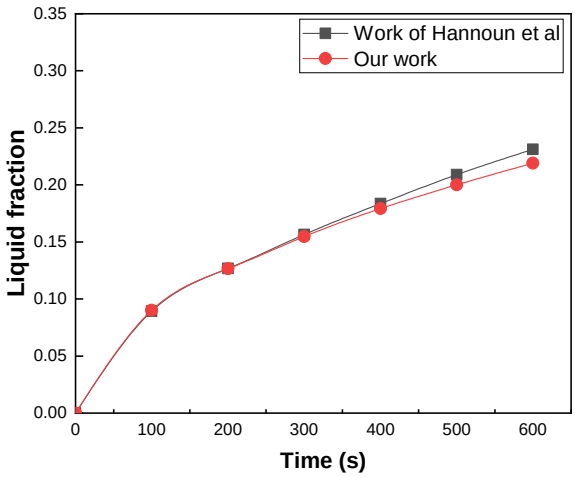

Figure 4. The temporal evolution of the liquid fraction

4.3 Time Step Effect

Performing a time-step examination is a critical aspect of any numerical study. In this specific phase of our research, the placement of (PCM) Outside the building enclosure was investigated, while the interior wall was constructed using a concrete layer. All cases, including the reference case, were subjected to identical imposed thermal conditions to ensure comprehensive comparability. To determine an appropriate time step for the simulations, three different time steps were used (Δt = 1, Δt = 0.5s, and Δt = 0.1s). The evaluation focused on the daily flux density in kWh/ m^2 from the interior wall, which directly interacts with the interior climate. As presented in Table 3, the results indicated few differences, with only 0.002% variance between the different time steps. Hence, based on this small discrepancy and to maintain computational efficiency, Δt = 1 s was chosen as the optimal time step for all subsequent calculations.

Table 3. Choice of time step

Time step Δt	Δt = 1 s	Δt = 0.5 s	Δt = 0.1 s
flow density [kWh/m^2]	-0.231815697	-0.231810861	-0.231810531
Max Deviation %	0.002%		

4.4 Thermal Behavior

To enhance heat transfer through wall integrating (PCMs), it is necessary to study their thermal behavior in depth during continuous exposure to an average heat flux over a 12-hour period. The graph in Fig. 5a-b shows the average temperatures observed for each wall examined, including the reference wall and those reinforced with external layers of PCMs of different types, at 6-hour and 12-hour intervals. In the case of a reference wall, external heat flow increases its temperature as heat propagates through the wall from the outer face to the inner face. Despite the wall's inherent inertia, which acts as a buffer for heat propagation, it fails to meet the required standards. It's important to note that the median temperature reaches 304 K after 6 hours and 314 K after 12 hours of exposure to an external heat flow. In contrast, incorporating selected PCM materials reveals a significant improvement in average temperatures. After 6 hours, the average temperature was recorded at 297.65 K for material A26, representing a significant drop of 7 degrees compared

with the reference wall. This result is superior to that of a study carried out by [37], which recorded a difference of just 3 degrees. It should be noted that the other two subjects recorded an increase of two degrees. Impressively, after 12 hours, the temperature of the wall containing the A26 reached 297.81 K, a significant reduction of 16 degrees compared with the reference wall. This reduction is significantly greater than that obtained in the study by [37] and in another study [38], which concluded that phase-change materials record a reduction of around 5 degrees when the PCM is solid and 8 degrees when it is liquid. Figure 5-b visually illustrates the contrast between the reference wall and the wall coated with PCM. Importantly, A26 stands out as the best PCM, showing greater temperature improvement than the other materials. This careful analysis confirms the effectiveness of A26 in improving thermal performance and provides valuable pointers for optimizing PCM-based wall systems to enhance heat transfer efficiency.

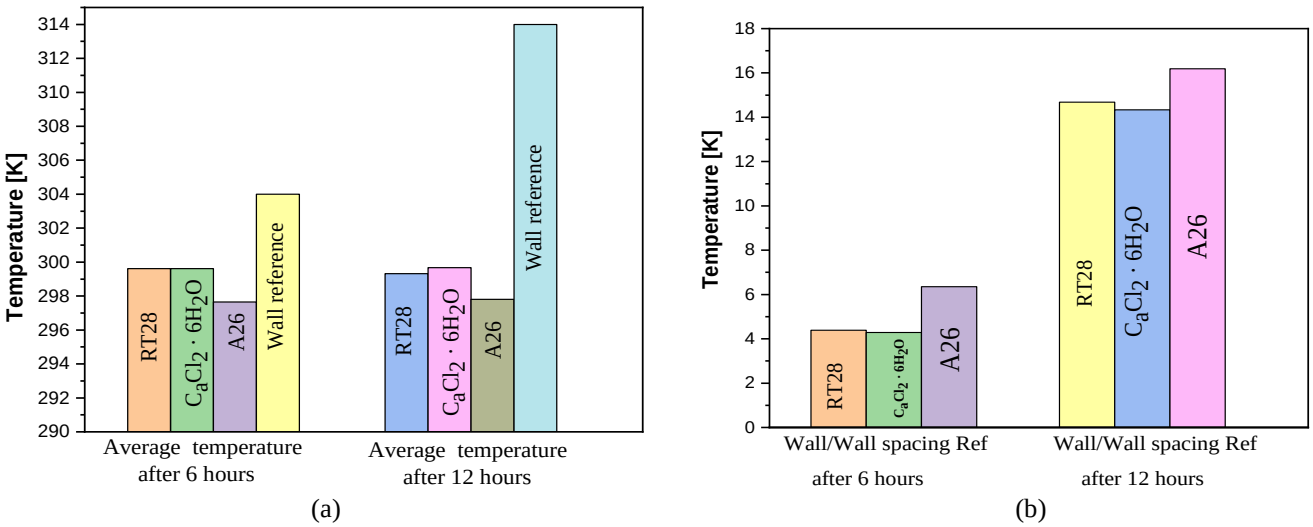

Figure 5. Average temperature values for the studied solutions. Average temperature for all solutions (a) Values of the difference between the reference neighbor and the wall with PCM (b)

To better understand heat transfer phenomena in walls containing phase-change materials (PCMs), it is essential to study their thermal behavior. This study exposes the aforementioned walls to an average heat flux for 12 hours. By visualizing the temperature dispersion throughout the wall thickness, the temperature profiles provide valuable information. Figures 6 show the 2D temperature distribution at $t = 6\ h$ and $t = 12\ h$ for different study cases. In the reference wall scenario, the external heat flow increases its temperature, causing heat to propagate towards the wall interior. This results in an average temperature of 304 K after 6 hours and 314 K after 12 hours of exposure to the external heat flux, consistent with the results in Figure 5. In the first case study, a layer of PCM is introduced on the external face to improve internal thermal comfort while maintaining a constant thickness for the wall. Figure 6 shows that all the cases studied show a reduction in average temperature values after 12 hours of exposure to the heat flow compared with the reference wall, with significant effectiveness observed in the wall containing A26. This wall, particularly the section containing PCM, shows intense interaction with heat, indicating significant heat absorption. This property effectively enables it to maintain thermal satisfaction and comfort within the building.

After observing that the addition of a (PCM) leads to a reduction in the average temperature of the concrete wall and that the disparity increases from 4.29°C to 16.19°C in contrast to the reference wall in the previous figures, the temporal evolution of the flux density on the interior surface of the wall is presented in Figure 7, with a constant temperature of 23 degrees Celsius. This figure covers the various cases studied (with and without PCM). In particular, the integration of PCMs has a significant impact on the flux density profile transmitted to the chamber. In addition, the wall incorporating fatty acid PCMs (A26) was observed to be particularly advantageous when considering an extrinsically arranged PCM layer. In absolute terms, the values for A26 show a significant reduction compared with the other selected materials. Table 4 summarizes these results, including the overall daily flux density and standard deviations of energy consumption for the PCM-equipped envelope compared to the reference wall. In terms of energy consumption, A26 fatty acid significantly reduces inward heat gain. This can be attributed to A26's low thermal diffusion and lower melting point than other materials. It should be noted that the flux density when using A26 is around 401 kW/m2, whereas this value doubles when using RT28 and the $CaCl_2.6H_2O$ salt. These observations underline the effectiveness of A26 in minimizing energy consumption and highlight its superiority over other PCM materials in the context of the thermal efficiency of the building envelopes.

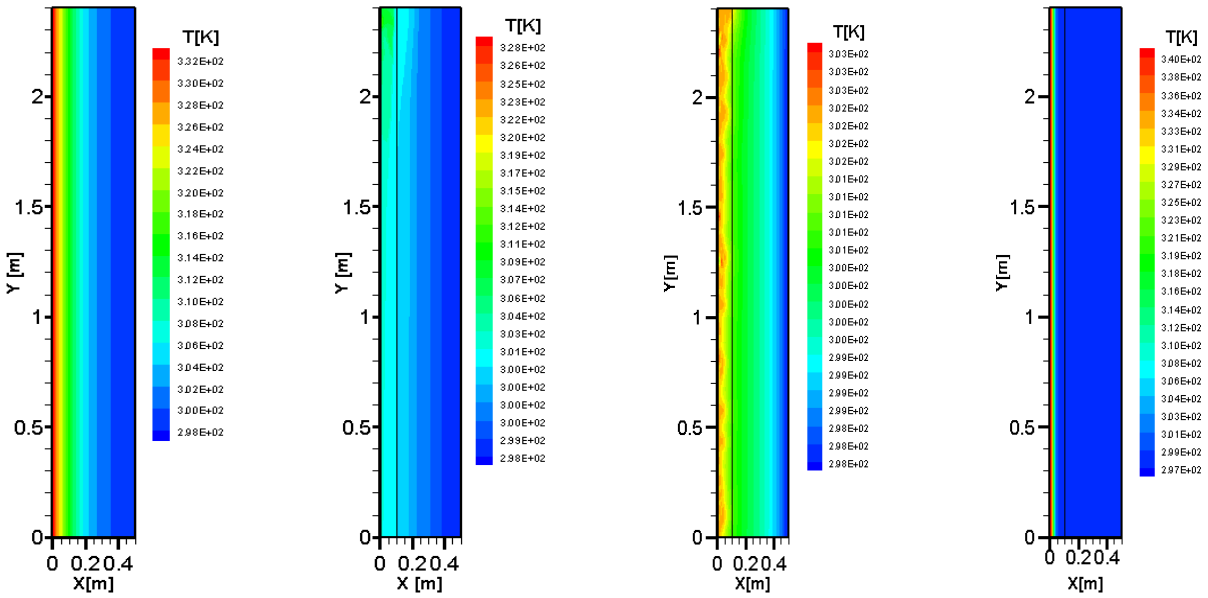

Reference wall | Wall with PCM-RT28 | Wall with PCM-Sel | Wall with PCM-A26

(a)

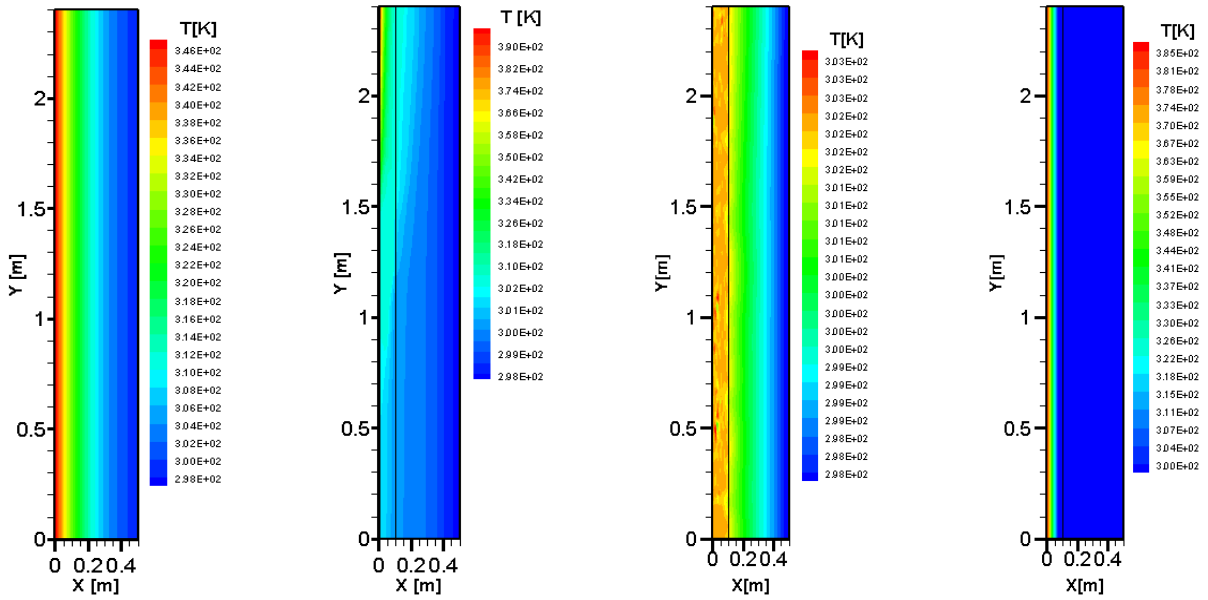

Reference wall | Wall with PCM-RT28 | Wall with PCM-Sel | Wall with PCM-A26

(b)

Figure 6. Contours of the isotherms: (a) after 6 hours, (b) after 12 hours

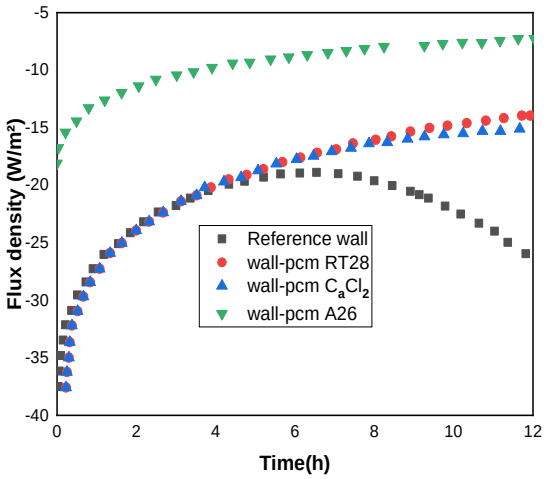

Figure 7. Comparison of the internal flows of the different cases

Table 4. The relative difference in energy consumption for different types of PCMs

Location external to the PCM	Reference wall	Paraffin RT28	Salt $CaCl_2 \cdot 6H_2O$	acid A26
flow density [W/m^2]	- 942986.1063	-834536.51	-839889.58	-401491.67
Flow density [kWh/m^2]	-0.26194	-0.23181	-0.2333	-0.111
$\boldsymbol{\sigma}$ %		11.5	10.95	57.42

4.5 Parametric Study and Discussion

To find the optimal PCM, the study cases are treated under the same conditions with the same objective: the calculation of the internal heat Flow involved. This quantity is compared to that of a reference wall, which will allow us to determine the optimal parameters that give us a minimum consumption of energy.

a) Optimal placement

In most previous research, the (PCM) stratum was often placed close to the indoor environment. An example is PCM-filled wallpaper attached to the interior wall surface [24]-[28]. In addition, other locations for the PCM layer have been investigated, such as near the outer wall surface [29]. The study of the best location for the PCM layer is crucial in construction, as it provides a better understanding of the heat transfer process. Numerical analyses were performed to ascertain the ideal placement of the PCM layer in the wall. In this part of the study, the initial parametric research focused on identifying the best position for the kerosene layer, in particular RT28 kerosene, in relation to the concrete wall. RT28 kerosene was selected for its preferred properties and habitat characteristics. Three distinct locations were considered: the external location (previously studied), the center of the wall, and the internal location directly connected to the room. Figure 8 provides a visual representation of the results of this parametric study.

Following the demonstration of the significance of the parametric study aimed at determining the optimal location for the Phase Change Material (PCM) layer, we now proceed to present the obtained results. Figure 9 illustrates the isotherms for all the studied configurations, including the PCM layer positioned externally, internally, and in the middle, along with the reference wall, after 6 and 12 hours. Additionally, Figure 10 provides a visualization of the liquid portion of the solutions. From the aforementioned study, the isotherm analysis after 6 and 12 hours reveals that the right portion of the wall (connected to the internal environment) is notably influenced by external heat flow, particularly evident after 12 hours when the PCM is situated externally and centrally (Figure 8). This observation aligns with the liquid portions of the PCM (Figure 10), where, after 12 hours of heat exposure, it is found that 80% of the PCM has melted, allowing convective heat to spread toward the wall. When the PCM is placed in the center, melting is only partial, and heat remains stagnant in the central region of the composite wall.

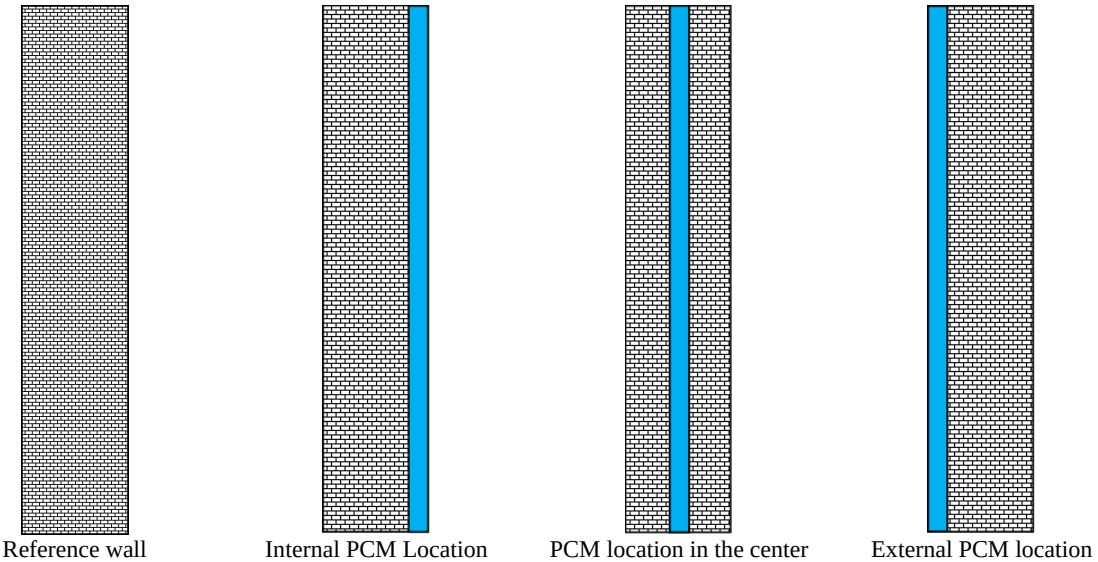

Figure 8. Different locations of the PCM layer (blue layer)

Conversely, when the PCM is placed on the inside, melting is negligible after 6 hours and minimal after 12 hours. Interestingly, placing the PCM layer inside the shell effectively prevents heat from spreading inwards, as all the energy stored in the PCM layer is used for the melting process. These findings may appear to contradict the results presented in the study [39], which suggested that the optimal situation is to place the PCM layer in the middle. However, it was also noted in [39] that placing the PCM layer on the inner side yields favorable results during peak times, reducing humidity and fostering a healthier environment. This assertion may slightly conflict with the study [40], whose proposal suggests

that the optimal position for the PCM layer is nearest to the outer surface. However, it acknowledges that the inner position becomes more favorable as the temperature of the inner surface rises. Despite these variations, all studies and the obtained results collectively affirm that the inner position of the PCM layer is distinctive and recommended, recognizing that results may vary based on boundary conditions. The earlier results align with the information presented in Table 5, which showcases energy consumption data and underscores that the optimal location is placing the PCM stratum internally. The internal location reduces consumption by approximately half, while alternative configurations (Positioning the PCM stratum centrally and externally) result in significantly lower percentage reductions. This condition will be the subject of studies dedicated to improving the depth of the PCM stratum in the interior portion.

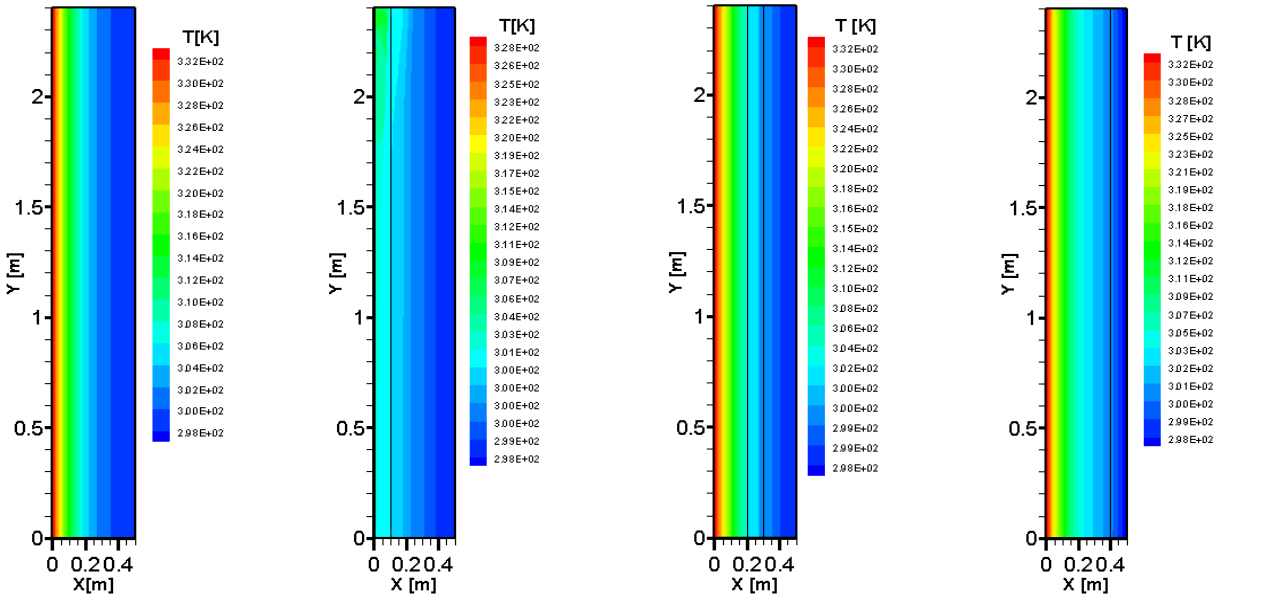

Reference wall 6h | Wall with PCM-external-RT28 | Wall with PCM-center-RT28 | Wall with PCM-internal-RT28

(a)

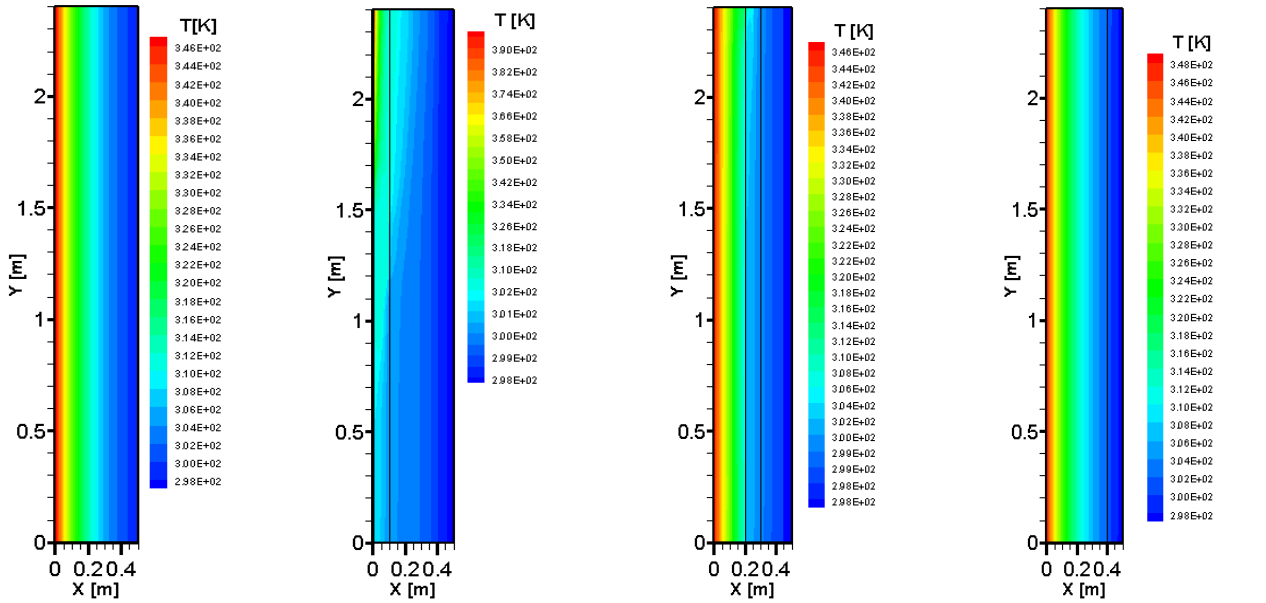

Reference wall | Wall with PCM-external-RT28 | Wall with PCM-center-RT28 | Wall with PCM-internal-RT28

(b)

Figure 9. Contours of the isotherms: (a) after 6 hours, (b) after 12 hours

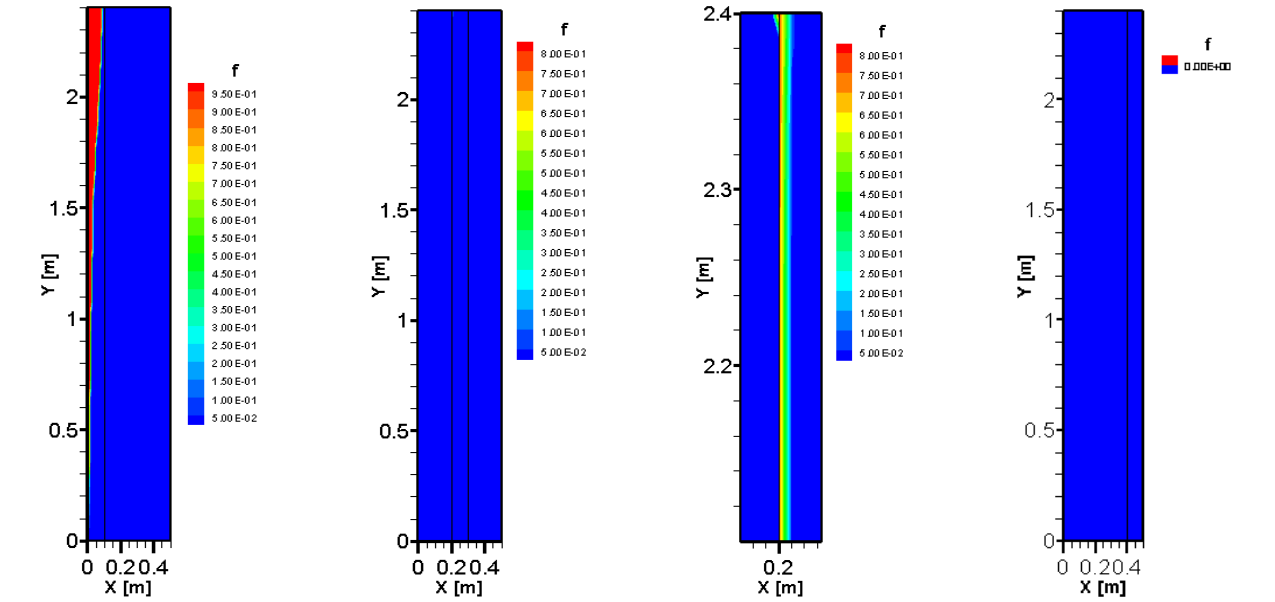

Wall with PCM-external-RT28 Wall with PCM-center-RT28 Wall with PCM-internal-RT28

(a)

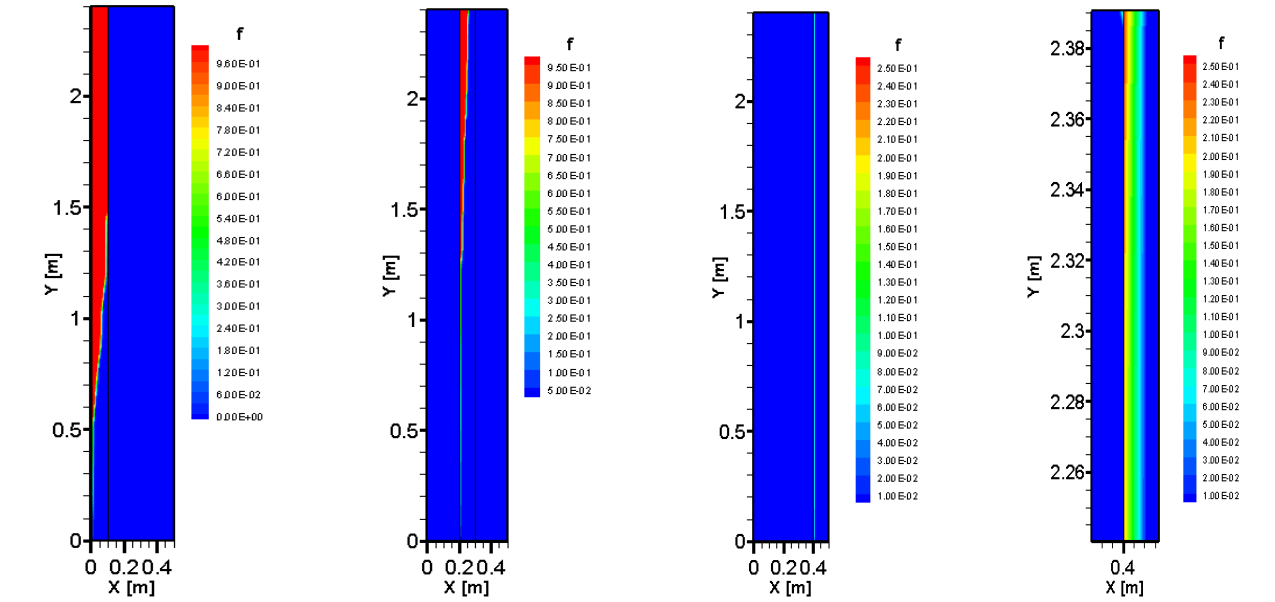

Wall with PCM-external-RT28 Wall with PCM-center-RT28 Wall with PCM-internal-RT28

(b)

Figure 10. The liquid fraction of PCM (RT28): (a) after 6 hours, (b) after 12 hours

Table 5. The relative difference in energy consumption for different locations of the PCM (RT28)

	Wall reference	PCM-RT28- external	PCM -RT28-center	PCM -RT28-internal
	- 942986.1063	-834536.51	-824992.5405	-466067.093
Flow density [kWh/m²]	-0.26194	-0.23181	-0.22916	-0.12946
Deviation % from the reference case		11.5	12.51	50.57

b) Optimal thickness

To conduct a more in-depth and impactful investigation, this section of the study seeks to examine the impact of the thickness of the phase change material (PCM) layer. Multiple thicknesses were examined to identify the optimal thickness while maintaining a consistent wall thickness of 50 cm. Table 6 provides an overview of the PCM layer thickness in conjunction with the corresponding concrete wall thickness, ensuring compatibility. The study is specifically conducted by situating the PCM stratum internally in the RT28 PCM stratum. The evolution of the heat flux density for each thickness of the PCM (RT28) over a 12-hour period is presented in Figure 11. Notably, the daily released heat flux exhibits

a significant decrease with increasing PCM stratum thickness. Additionally, it is observed that the total flux density decreases after 8 hours for lower thicknesses while it increases for higher thicknesses. This phenomenon can be ascribed to the slender stratum of PCM receiving heat flux from the wall, increasing its temperature until it attains the melting point. The total flux density transmitted to the inside remains fairly consistent during the phase change of the PCM., occurring between 3 and 7 hours. Once melting is complete, the total flux density transferred inward increases in absolute value compared to other thicknesses, or the PCM continues to melt after 8 hours of exposure to the heat flux. Examining the energy consumption aspect, Figure 12 illustrates a decrease of 28.0% (E1), 42.0% (E2), 49.0% (E3), and 52.0% (E4). Beyond a thickness of 15.0 cm, the flux decrease remains constant. The results suggest that the optimum thickness for the RT28 PCM stratum is between 10 and 15 cm. These results offer valuable insights into optimizing the thermal performance of PCM-based wall systems, particularly with regard to thickness considerations.

Table 6. The thicknesses of the PCM stratum (layer)

Thickness of the PCM stratum	Wall thickness
Thickness of the PCM layer [*cm*]	Normal concrete[*cm*]
2.5	47.5
5.0	45.0
10.0	40.0
15.0	35.0
20.0	30.0
25.0	25.0

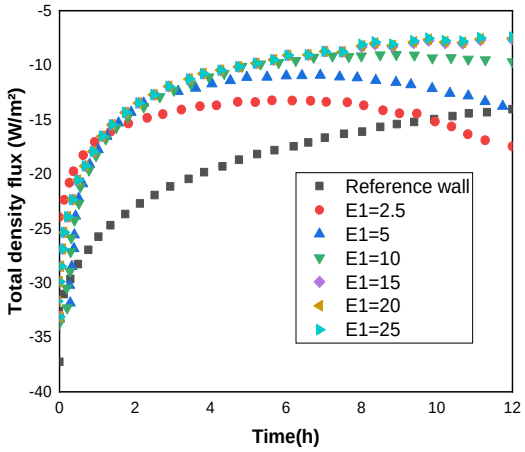

Figure 11. Evolution of the heat flow density for the duration of 12 hours for each thickness of the PCM (RT28)

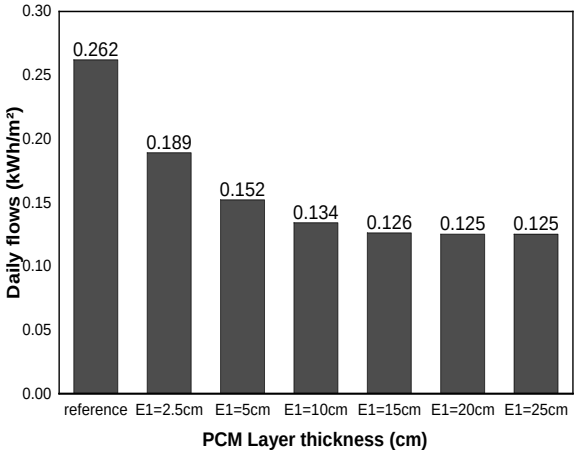

Figure 12. Histogram of daily flows for each thickness of the PCM (RT28)

c) Flow effect

In pursuit of a comprehensive understanding of the boundary conditions and their impact on the Phase Change Material (PCM) layer, various heat flow values on the outer face were incrementally elevated (350, 400, 450, 500, 550, and 600 W/m2). This experimentation was conducted while maintaining the wall installed with the PCM stratum (layer)in

contact with the inner part of the room and possessing a consistent thickness of 10 cm. Figure 13 vividly portrays the effect of the increased heat flow imposed on the outer face of the wall, specifically focusing on the liquid portion of the PCM over time. Table **7** provides a detailed summary of the influence of the external heat flow. Notably, the table underscores that the internal flow across the inner surface of the PCM remains consistent throughout the entire 12-hour period. This constancy can be attributed to the PCM's melting period.

Moreover, Figure 13 visually demonstrates that the liquid percentage exhibits an increasing trend in response to the heat flow with stable fluid values for 8 hours, reaching 0.025 after 12 hours across various chosen flow values. Analyzing the efficacy of PCM (RT28) in decreasing heat flow to the interior, a notable reduction of approximately 50.60% is observed. Remarkably, the increase in external heat flux does not significantly impact this reduction, with the difference not exceeding 1% of the calculated value (Table **7**). These findings emphasize the robustness of PCM (RT28) in maintaining consistent heat flow reduction, even when exposed to varying external heat flux conditions. The intricate interplay between external heat inputs and PCM performance contributes to a nuanced understanding of the dynamic thermal behavior within building envelopes.

Table **7**. Effect of external heat flow

	Reference wall	Φ=350 *W/m²*	Φ=400 *W/m²*	Φ=450 *W/m²*	Φ=500 *W/m²*	Φ=550 *W/m²*	Φ=600 *W/m²*
Flow density [*kWh/m²*]	-0.26194	-0.12946	-0.12979	-0.13008	-0.13033	-0.13056	-0.13077
Deviation % from the reference case		50.57	50.45	50.34	50.24	50.15	50.07

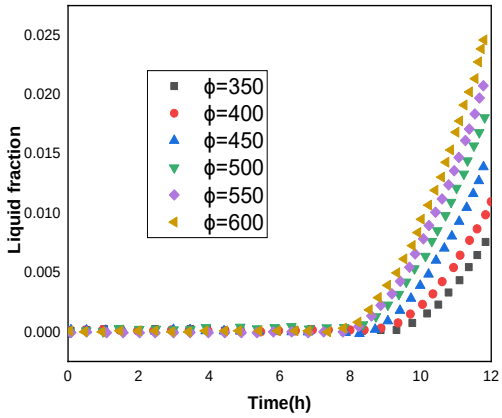

Figure 13. Effect of increasing the imposed heat flow on the outer face of the wall (liquid fraction of the PCM)

5.0 CONCLUSIONS

This study presented a computational analysis using the commercial program "Fluent 14.0" to explore the integration of PCMs in the wall to improve internal thermal satisfaction (thermal comfort). A reference wall and a wall composed of a PCM stratum (layer) and a regular concrete layer were investigated, and both were subjected to the same thermal conditions. Three types of PCM were analyzed, namely RT28 kerosene, $CaCl_2.6H_2O$ hydrated salt, and A26 fatty acid. The study revealed that positioning the fatty acid in the outer part of the envelope reduced energy consumption by 50% in comparison with the baseline wall. In addition, it showed that placing the RT28 PCM in the inner part of the wall, in touch with the internal environment, further optimized energy efficiency and led to a 50% reduction in energy consumption.

The investigation conducted on a reference wall and a wall comprised of a PCM stratum and a standard concrete layer, both under identical thermal conditions, deepened our understanding of the integration of PCMs into the wall. Our findings suggest that the optimal depth of the PCM layer ranges from 10 cm to 15 cm. Moreover, it was observed that increasing the external heat flow affects the liquid fraction of the PCM, which rises steadily at a fixed temperature. Meanwhile, the heat flow to the interior stays constant.

The discoveries from this study lay the groundwork for forthcoming research and exploration. It is suggested that future work involves the integration of this wall into a living room cavity and the analysis of the dynamics and thermal behavior of unsteady flow. Additionally, it is recommended that other phase change materials be explored to determine the optimal option and incorporate PCM into the floor and ceiling for a more comprehensive approach.

This study aims to contribute to a sustainable and environmentally conscious building sector. This will be achieved through a comprehensive examination and synthesis of existing literature on PCM technology and its impact on enhancing

energy efficiency in construction. The discoveries of this study have the potential to inform and guide future endeavors in promoting environmentally friendly practices within the building industry.

Nomenclature

$\boldsymbol{\phi_{cv,p}}$	Convective flow density inside the wall	*[W/ m^2]*
$\boldsymbol{h_{int}}$	Interior convective exchange coefficient	*[W/ m^2.K]*
$\mathbf{T_{si,p}}$	Inner wall surface temperature	*[K]*
$\mathbf{T_{int}}$	Indoor air temperature	*[K]*
H	Enthalpy	*[J/Kg]*
ρ	Masse volumique density	*[Kg/m^3]*
v	Fluid velocity	*[m/s]*
h	Sensible enthalpy	*[J/m^3]*
$\mathbf{h_{ref}}$	Reference enthalpy	*[J/m^3]*
$\mathbf{T_{ref}}$	Reference temperature	*[K]*
$\mathbf{C_p}$	Specific heat at constant pressure of PCM	*[J/Kg.K]*
L	Latent heat of PCM	*[J/Kg]*
$\mathbf{T_{solidus}}$ $\mathbf{T_{liquidus}}$	PCM solidification and liquefaction temperatures	*[K]*

6.0 ACKNOWLEDGEMENT

The authors express their sincere gratitude to the University of Oum El Bouaghi, Algeria, and the Laboratory of Advanced Design and Modeling of Mechanical and Thermo-Fluid Systems (LCMASMTF) for their invaluable support throughout the research process.

7.0 REFERENCES

[1] P. Tatsidjodoung, N. Le Pierrès, and L. Luo, "A review of potential materials for thermal energy storage in building applications," *Renewable and Sustainable Energy Reviews*, vol. 18. pp. 327–349, 2013.

[2] A. Waqas and Z. Ud Din, "Phase change material (PCM) storage for free cooling of buildings - A review," *Renewable and Sustainable Energy Reviews*, vol. 18. pp. 607–625, 2013.

[3] *Energie dans les zones*. APRUE, 2015.

[4] A. M. Khudhair and M. M. Farid, "A review on energy conservation in building applications with thermal storage by latent heat using phase change materials," *Energy Conversion and Management*, vol. 45, no. 2, pp. 263–275, 2004.

[5] L. F. Cabeza, A. Castell, C. Barreneche, A. De Gracia, and A. I. Fernández, "Materials used as PCM in thermal energy storage in buildings: A review," *Renewable and Sustainable Energy Reviews*, vol. 15, no. 3. pp. 1675–1695, 2011.

[6] T. Nomura, N. Okinaka, and T. Akiyama, "Technology of latent heat storage for high temperature application: A review," *Iron and Steel Institute of Japan International*, vol. 50, no. 9, pp. 1229–1239, 2010.

[7] R. Baetens, B. P. Jelle, and A. Gustavsen, "Phase change materials for building applications: A state-of-the-art review," *Energy and Buildings*, vol. 42, no. 9, pp. 1361–1368, 2010.

[8] F. Agyenim, N. Hewitt, P. Eames, and M. Smyth, "A review of materials, heat transfer and phase change problem formulation for latent heat thermal energy storage systems (LHTESS)," *Renewable and Sustainable Energy Reviews*, vol. 14, no. 2. pp. 615–628, Feb. 2010.

[9] A. F. Regin, S. C. Solanki, and J. S. Saini, "Heat transfer characteristics of thermal energy storage system using PCM capsules: A review," *Renewable and Sustainable Energy Reviews*, vol. 12, no. 9, pp. 2438–2458, 2008.

[10] M. M. Farid, A. M. Khudhair, S. A. K. Razack, and S. Al-Hallaj, "A review on phase change energy storage: Materials and applications," *Energy Conversion and Management*, vol. 45, no. 9–10. pp. 1597–1615, 2004.

[11] J. Xie, W. Wang, J. Liu, and S. Pan, "Thermal performance analysis of PCM wallboards for building application based on numerical simulation," *Solar Energy*, vol. 162, pp. 533–540, 2018.

[12] P. Wang, Z. Liu, S. Xi, Y. Zhang, and L. Zhang, "Experiment and numerical simulation of an adaptive building roof combining variable transparency shape-stabilized PCM," *Energy and Buildings*, vol. 263, 2022.

[13] N. Soares, A. Samagaio, R. Vicente, and J. Costa, "Numerical Simulation of a PCM Shutter for Buildings Space Heating During the Winter," in *Proceedings of the World Renewable Energy Congress – Sweden, 8–13 May, 2011, Linköping, Sweden*, Linköping University Electronic Press, Nov. 2011, pp. 1797–1804.

[14] K. Biswas, Y. Shukla, A. Desjarlais, and R. Rawal, "Thermal characterization of full-scale PCM products and numerical simulations, including hysteresis, to evaluate energy impacts in an envelope application," *Applied Thermal Engineering*, vol. 138, pp. 501–512, 2018.

[15] J. K. Kissock, J. M. Hannig, T. I. Whitney, and M. L. Drake, "Testing and simulation of phase change wallboard for thermal storage in buildings," *Solar Engineering*, pp. 45–52, 1998.

[16] K. Kissock and S. Limas, "Diurnal load reduction through phase-change building components," *ASHRAE Transactions*, vol. 112, no. 1, 2006.

[17] V. V. Tyagi and D. Buddhi, "PCM thermal storage in buildings: A state of art," *Renewable and Sustainable Energy Reviews*, vol. 11, no. 6. pp. 1146–1166, 2007.

[18] F. Kuznik, D. David, K. Johannes, and J. J. Roux, "A review on phase change materials integrated in building walls," *Renewable and Sustainable Energy Reviews*, vol. 15, no. 1, pp. 379–391, 2011.

[19] D. Zhou, C. Y. Zhao, and Y. Tian, "Review on thermal energy storage with phase change materials (PCMs) in building applications," *Applied Energy*, vol. 92, pp. 593–605, 2012.

[20] V. V. Tyagi, S. C. Kaushik, S. K. Tyagi, and T. Akiyama, "Development of phase change materials based microencapsulated technology for buildings: A review," *Renewable and Sustainable Energy Reviews*, vol. 15, no. 2. pp. 1373–1391, 2011.

[21] P. B. Salunkhe and P. S. Shembekar, "A review on effect of phase change material encapsulation on the thermal performance of a system," *Renewable and Sustainable Energy Reviews*, vol. 16, no. 8. pp. 5603–5616, 2012.

[22] T. C. Ling and C. S. Poon, "Use of phase change materials for thermal energy storage in concrete: An overview," *Construction and Building Materials*, vol. 46. pp. 55–62, 2013.

[23] M. Hunger, A. G. Entrop, I. Mandilaras, H. J. H. Brouwers, and M. Founti, "The behavior of self-compacting concrete containing micro-encapsulated Phase Change Materials," *Cement and Concrete Composites*, vol. 31, no. 10, pp. 731–743, 2009.

[24] I. Mandilaras, M. Stamatiadou, D. Katsourinis, G. Zannis, and M. Founti, "Experimental thermal characterization of a Mediterranean residential building with PCM gypsum board walls," *Building and Environment*, vol. 61, pp. 93–103, 2013.

[25] A. V. Sá, M. Azenha, H. De Sousa, and A. Samagaio, "Thermal enhancement of plastering mortars with Phase Change Materials: Experimental and numerical approach," *Energy and Buildings*, vol. 49. pp. 16–27, 2012.

[26] C. Voelker, O. Kornadt, and M. Ostry, "Temperature reduction due to the application of phase change materials," *Energy and Buildings*, vol. 40, no. 5, pp. 937–944, 2008.

[27] B. M. Diaconu, "Thermal energy savings in buildings with PCM-enhanced envelope: Influence of occupancy pattern and ventilation," *Energy and Buildings*, vol. 43, no. 1, pp. 101–107, 2011.

[28] G. Zhou, Y. Yang, X. Wang, and S. Zhou, "Numerical analysis of effect of shape-stabilized phase change material plates in a building combined with night ventilation," *Applied Energy*, vol. 86, no. 1, pp. 52–59, 2009.

[29] M. D. Romero-Sánchez, C. Guillem-López, A. M. Lopez-Buendia, M. Stamatiadou, I. D. Mandilaras, D. Katsourinis et al., "Treatment of natural stones with Phase Change Materials: Experiments and computational approaches," *Applied Thermal Engineering*, vol. 48, pp. 136–143, 2012.

[30] X. Jin, M. A. Medina, and X. Zhang, "On the importance of the location of PCMs in building walls for enhanced thermal performance," *Applied Energy*, vol. 106, pp. 72–78, 2013.

[31] J. E. Matsson, *An Introduction to Ansys Fluent 2023*. Sdc Publications, 2023.

[32] M. A. Hassab, M. M. Sorour, M. Khamis Mansour, and M. M. Zaytoun, "Effect of volume expansion on the melting process"s thermal behavior," *Applied Thermal Engineering*, vol. 115, pp. 350–362, 2017.

[33] M. Arıcı, E. Tütüncü, M. Kan, and H. Karabay, "Melting of nanoparticle-enhanced paraffin wax in a rectangular enclosure with partially active walls," *International Journal of Heat and Mass Transfer*, vol. 104, pp. 7–17, Jan. 2017.

[34] "ANSI/ASHRAE Standard 55-2023, Thermal Environmental Conditions for Human Occupancy," *American Society of Heating, Refrigerating and Air-Conditioning Engineers*. 2023. [Online]. Available: www.ashrae.org

[35] DTR C3.2/4, "Document Technique Réglementaire, Règlementation Thermique Algérienne du Bâtiment," *CNERIB*. 2016.

[36] N. Hannoun, V. Alexiades, and T. Z. Mai, "A reference solution for phase change with convection," *International Journal for Numerical Methods in Fluids*, vol. 48, pp. 1283–1308, 2005.

[37] L. F. Cabeza, C. Castellón, M. Nogués, M. Medrano, R. Leppers, and O. Zubillaga, "Use of microencapsulated PCM in concrete walls for energy savings," *Energy and Buildings*, vol. 39, no. 2, pp. 113–119, 2007.

[38] L. F. Cabeza, L. Navarro, A. L. Pisello, L. Olivieri, C. Bartolomé, J. S. Ramos et al., "Behaviour of a concrete wall containing micro-encapsulated PCM after a decade of its construction," *Solar Energy*, vol. 200, pp. 108–113, 2020.

[39] X. Shi, S. A. Memon, W. Tang, H. Cui, and F. Xing, "Experimental assessment of position of macro encapsulated phase change material in concrete walls on indoor temperatures and humidity levels," *Energy and Buildings*, vol. 71, pp. 80–87, 2014.

[40] X. Jin, M. A. Medina, and X. Zhang, "Numerical analysis for the optimal location of a thin PCM layer in frame walls," *Applied Thermal Engineering*, vol. 103, pp. 1057–1063, 2016.